Matching convolved images to optically blurred images on the retina

Sara Aissati Instituto de Óptica 'Daza de Valdés', Consejo Superior de Investigaciones Científicas, CSIC, Madrid, Spain

Clara Benedi-Garcia Instituto de Óptica 'Daza de Valdés', Consejo Superior de Investigaciones Científicas, CSIC, Madrid, Spain

Maria Vinas Wellman Center for Photomedicine, Massachusetts General Hospital, Harvard Medical School, Boston, MA, USA

Alberto de Castro Instituto de Óptica 'Daza de Valdés', Consejo Superior de Investigaciones Científicas, CSIC, Madrid, Spain

Susana Marcos Center for Visual Science, The Institute of Optics and Flaum Eye Institute, University of Rochester, NY, USA
Instituto de Óptica 'Daza de Valdés', Consejo Superior de Investigaciones Científicas, CSIC, Madrid, Spain

Convolved images are often used to simulate the effect of ocular aberrations on image quality, where the retinal image is simulated by convolving the stimulus with the point spread function derived from the subject's aberrations. However, some studies have shown that convolved images are perceived far more degraded than the same image blurred with optical defocus. We hypothesized that the positive interactions between the monochromatic and chromatic aberrations in the eye are lost in the convolution process. To test this hypothesis, we evaluated optical and visual quality with natural optics and with convolved images (on-bench, computer simulations, and visual acuity [VA] in subjects) using a polychromatic adaptive optics system with monochromatic (555 nm) and polychromatic light (WL) illumination. The subject's aberrations were measured using a Hartmann Shack system and were used to convolve the visual stimuli, using Fourier optics. The convolved images were seen through corrected optics. VA with convolved stimuli was lower than VA through natural aberrations, particularly in WL (by 26% in WL). Our results suggest that the systematic decrease in visual performance with visual acuity and retinal image quality by simulation with convolved stimuli appears to be primarily associated with a lack of favorable interaction between chromatic and monochromatic aberrations in the eye.

Introduction

The optics of the eye projects a degraded image on the retina. Adaptive optics (AO) has become a suitable technique to correct or manipulate the ocular high-order aberrations (HOAs), therefore modifying the form and magnitude of retinal blur (Marcos et al., 2017). AO systems are generally provided with an active element working in a closed-loop operation, such that the combined wave aberration of the AO mirror plus the eye's optics is nearly diffraction limited. Correction of HOAs has been shown to result in improved visual acuity (Marcos et al., 2008) and contrast sensitivity (Dalimier et al., 2008; de Gracia et al., 2011) and to improve certain visual tasks such as familiar face recognition (Sawides et al., 2010).

Resorting to Fourier optics is a common practice to illustrate the retinal image quality and to investigate the first step in the visual process. In this method, simulations of the images of an external object projected on the retina are obtained by the convolution of the original image ("object") with the ocular point spread function (PSF).

The PSF can be either measured experimentally from double-pass retinal images or calculated from the measured wave aberration. Estimations of the PSF of the eye include classical work by Flamant (1955), in

Citation: Aissati, S., Benedi-Garcia, C., Vinas, M., de Castro, A., & Marcos, S. (2022). Matching convolved images to optically blurred images on the retina. *Journal of Vision*, *22*(2):12, 1–14, https://doi.org/10.1167/jov.22.2.12.

https://doi.org/10.1167/jov.22.2.12 Received August 17, 2021; published February 18, 2022 ISSN 1534-7362

which the light distribution curves in the retina were obtained using a slit of light to calculate the line spread function, and Santamaria et al. (1987) and Artal et al. (1995), who reported the first double-pass PSF from human eyes at the Institute of Optics of the Spanish National Research Council (IO-CSIC) in Madrid.

The use of mathematical convolution to represent retinal images or to evaluate the effects of individual aberration terms on image quality has been extensively used in the literature (Burton & Haig, 1984; Artal, 1990; Applegate et al., 2003). In a seminal paper, Artal (1990) presented the first calculations of two-dimensional (2-D) extended foveal images using experimental double-pass PSFs. More recently, the PSF used in convolution has been calculated from the wave aberration, as the Fourier transform of the pupil function, where the phase is the wavefront aberration and the modulus is the transmittance of the optical system.

The convolution calculations are often used to illustrate differences in the retinal image quality across patients with different aberration profiles (Applegate et al., 2002), different treatments (e.g., intraocular lenses on different eyes; Marcos et al., 2005), or across the peripheral retina in the same subject (Jaeken & Artal, 2012). Some authors have projected synthetic images (by convolution) on the subject's retina, trying to minimize the impact of the natural optics of the eye. Applegate et al. (2003) presented visual acuity charts degraded by the subject's aberrations through a 3-mm artificial pupil size, assuming that this pupil diameter represents a good trade-off between diffraction and aberrations (Charman, 1991). Peli and Lang (2001) tested experimentally the degradation of a multifocal intraocular lens (IOL) in eyes monolaterally implanted with a multifocal IOL. They filtered the images with the optical transfer function (OTF) of the eye equipped with a multifocal IOL (divided by the OTF of the monofocal IOL) and presented them to the contralateral eye with a monofocal IOL for intereye comparison. Legras et al. (2004) predicted retinal images with various levels of defocus by convolution and compared them with real defocused images with trial lenses for different pupil diameters and monochromatic and polychromatic light. Various studies used convolved images to simulate different amounts and orientations of blur in psychophysical studies (Sawides et al., 2011a; Sawides et al., 2011b).

Previous works have used different strategies to minimize further degradation of the convolved stimulus viewed through the subject's optics, either using deconvolution with the observing optics, inverse filters, and reduction of the size of the observing pupil or, more recently, using adaptive optics to correct the eye's aberrations.

Despite the common use of convolved images to represent the retinal image quality, the underlying assumptions of this approach have been little explored. In fact, recent studies report significant differences in visual acuity (VA) assessed with simulated stimuli as opposed to optical manipulation of the aberration pattern in natural viewing (de Gracia et al., 2009). In more recent work, Ohlendorf et al. (2011) found that VA was worse with simulated spherical error and considerably worse with simulated astigmatic defocus than with real optical defocus of the same magnitudes. The origin of the discrepancies could not be explained.

Two factors have been argued to potentially affect differently the quality of convolved images projected on the retina through diffraction-limited optics and the quality of images directly degraded by the optics: the Stiles–Crawford effect (SCE) and the chromatic aberration. The SCE is often modeled as an apodized pupil. Some studies anticipate that the attenuation of the impact of the peripheral aberrations produced by pupil apodization may potentially improve the retinal image over constant amplitude in the pupil function (Applegate & Lakshminarayanan, 1993; He et al., 1999). However, except for some experimental studies artificially shifting the peak location of the Stiles–Crawford function by filters that showed a small impact on the modulation transfer function (MTF) and visual performance (van Meeteren, 1974; Atchison et al., 2003; Marcos & Burns, 2009), there is little evidence that the Stiles–Crawford profile produces a significant impact on the retinal image quality (Atchison et al., 1998; Burns & Marcos, 2000; Atchison et al., 2003).

The other potential contributor to a discrepancy between the convolved image and the real optical image projected on the retina is chromatic aberration. Convolved images are commonly generated using a monochromatic PSF (Ravikumar et al., 2008). However, images, even if projected through diffraction-limited optics, are subject to the chromatic aberration of the eye. Previous work has shown that in fact, the effect of chromatic aberration is more deleterious to vision under perfect optics than under uncorrected aberrations (McLellan et al., 2002; Benedi-Garcia et al., 2021). Under this hypothesis, the convolved images seen through AO-corrected optics would produce the same retinal image as natural images seen through the aberrations of the eye. However, in polychromatic light, with AO, chromatic aberrations are still present, and possible favorable interactions between chromatic and monochromatic aberrations would be attenuated.

The purpose of this study is to evaluate to what extent the optical and visual acuity with convolved stimuli is comparable to those obtained with natural optical aberrations in monochromatic and polychromatic light. Understanding the discrepancy that exists between the images seen through the natural aberrations of the subject and convolved images opens up a breadth of possibilities for simulating different conditions and studying retinal quality through the subject's natural

optics. For example, it would be possible to provide the experience of intraocular lens or contact lens designs, refractive surgery patterns, or individual aberrations without the need of complex optical elements for simulation.

Methods

A polychromatic AO system was used to measure and correct the HOAs of seven subjects. Measurements were performed with high-contrast stimuli seen under natural optics and with convolved stimuli (degraded by the subject's aberrations) seen under AO-corrected optics. Computational simulations and on-bench measurements were performed to evaluate the effect solely on optical grounds. Measurements of visual acuity and computer simulations were done for monochromatic and polychromatic stimuli to evaluate the effect of chromatic aberration.

Polychromatic adaptive optics system

A custom-developed polychromatic AO system at the Visual Optics and Biophotonics Lab (Institute of Optics, Spanish National Research Council, IO-CSIC, Madrid, Spain) was used in this study to correct the subject's aberrations and to induce aberrations in on-bench control experiments. The system and all its channels have been described in detail in previous publications (Vinas et al., 2015; Marcos et al., 2017; Vinas, Aissati, et al., 2019; Vinas, Benedi-Garcia, et al., 2019; Aissati et al., 2020; Marcos et al., 2020; Vinas et al., 2020). The main channels used in this study of the system are as follows:

1. The illumination channel, composed of a Supercontinuum Laser Source (SCLS, SC400 femtopower 1060 supercontinuum laser; Fianium Ltd, Southampton, United Kingdom, UK), in combination with an acusto-optic tunable filter (AOTF) module (FYLA LASER S.L, Valencia, Spain), which is controlled by radiofrequency drivers and selects the appropriate wavelength in visible light automatically (450–700 nm). For the purposes of this study, a 555-nm wavelength (12 nm bandwidth) was used to illuminate visual stimuli. A Super Luminescent Diode (SLD, Superlum, Munster, Ireland) coupled to an optical fiber emitting at 880 nm was used to measure the HOAs. In all cases, the maximum power reaching the eye was at least one order of magnitude below the safety limits prescribed by the American National Standard Institute for all wavelengths used in the experiments (Delori et al., 2007).
2. AO control channel composed by a Hartmann–Shack wavefront sensor (HS) and an electromagnetic deformable mirror (DM). The HS (HASO 32 OEM; Imagine Eyes, Orsay, France) is composed of an array of 40 × 32 microlenses. The DM (52 actuators, a 15-mm effective diameter and a 50-µm stroke; MIRAO, Imagine Eyes) works in a closed loop with the HS to correct the system's and eye's aberrations, as well as to induce aberrations (which is the purpose of this study). The HS and the DM were placed on conjugated pupil planes. Aberrations were fitted by Zernike polynomials up to 37 terms (seventh order), with notation following the recommendations of the OSA (Optical Society of America) Standard Committee (Thibos et al., 2000).
3. The psychophysical channel contained a Digital Micro-Mirror device (DMD; DLP Discovery 4100 0.7 XGA; Texas Instruments Incorporated, Dallas, Texas, USA). The DMD was located in a conjugate retinal plane and was used to display visual stimuli subtending 1.62 angular degrees. The DMD was illuminated either monochromatically (555 nm) or with a white light source (WL; Halogen Fiber Light Sources LQ, Output Power 20–250 W, 3,000–3,400 K, Linos; Qioptiq, Rhyl, UK). The power and the spectrum of the source were characterized with a spectrometer (USB4000-Fiber Optic Spectrometer, 200–1,100 nm; Ocean Optics, Florida, USA) before conducting the experiment. The luminance of the stimulus on the retinal plane was 20–25 cd/m^2 for both light sources and therefore in the photopic region. The luminance of the WL was adjusted perceptually to match that of the SCLS 555-nm light in a psychophysical equiluminance test (Anstis & Cavanagh, 1983; Raphael & MacLeod, 2011; Benedi-Garcia et al., 2021). The value of the neutral density filter was chosen from the average of the settings of five subjects.
4. The Badal optometer (formed by two lenses of a 125-mm focal distance) allows compensating for the spherical error of the eye without changing the magnification.
5. Natural pupil monitoring system, consisting of an infrared (IR) camera conjugated to the eye's pupil.

All optoelectronic elements of the system (SCLS main source, AOTF, Badal system, pupil cameras, HS wavefront sensor, deformable mirror, and DMD) were automatically controlled and synchronized using ready-made or custom-built software programmed in Visual C++ and C# (Microsoft, Redmond, WA, USA) and MATLAB (MathWorks, Natick, MA, USA).

Convolved images

Convolved images were generated using standard Fourier optics (Goodman, 1996). Simulated degraded

stimuli of E-letters were used in both on-bench experiments where the stimuli were projected on the CCD camera acting as an artificial "retina" in an artificial eye and the VA tests in patients.

The Snellen E-letter stimuli for the visual acuity psychophysical tests ranged between 0.20 and 49.05 arcmin angular subtended (which corresponded to −1.3 logMAR to 1.1 logMAR). The Snellen E-letter used in on-bench experiments subtended 19.62 arcmin (which corresponded to 0.7 logMAR). The PSFs were computed from the ocular aberrations (previously measured with the HS) of each participating subject, as well as from the residual aberrations after adaptive optics correction. Calculations were performed using the fast Fourier optics function (fft2) in MATLAB. The scale of PSFs was calculated to match the pixel/angular scale of the stimulus object, according to the viewing conditions, size of the stimulus, and magnification of the system. The retinal image was simulated as the convolution of the PSF and the object (Equation 1), using the "conv2" function in MATLAB.

$$Image = PSF_{555nm} \otimes Object \quad (1)$$

The total energy of the stimulus ("object") and the energy of the final convolved image must be preserved after the convolution. Thus, the sum of the total energy of the PSF with the aberrations of the subjects was normalized to 1.

Computational calculations were performed for 6-mm pupils and a monochromatic wavelength of 555 nm, replicating the experimental conditions, unless otherwise noted. The sets of Zernike terms to calculate the PSF were obtained from measurements with the HS wavefront sensor (wavefront fit up to a seventh-order term). Piston and tilts were ignored. Convolved images were simulated for optimal focus, estimated as the defocus term that optimized a visual Strehl (VS) (Iskander, 2006) metric in a through-focus range (from −4.00 to 4.00 D in 0.01-D steps). The original images (E-letters) were high-contrast images (binary images contained only one bit per pixel to represent two gray values, 0 [black] and 1 [white]). The calculations were performed prior to the on-bench or the VA measurements. The DMD was linearized with the calibrated gamma curve.

On-bench testing

The experimental measurement was mimicked with the deformable mirror and an artificial eye. The artificial eye consisted of a 50.8-mm focal length achromatic doublet lens and a CCD camera (DCC1240C—High-Sensitivity USB 2.0 CMOS Camera, 1,280 × 1,024, Global Shutter, Color Sensor; Thorlabs GmbH, Munich, Germany) acting as an artificial "retina" and was placed in the AO system in the position of the subject's eye. The aberrations of the subjects were mapped in the DM to simulate the condition of optical degradation by the eye's aberrations. In this condition, the Badal optometer was set to the defocus position that maximized the VS for each set of aberrations. Conversely, the DM was set to correct all the aberrations of the optical system and the artificial eye, and convolved images (simulated using the subject's aberrations) were projected on the retina of the artificial eye through fully corrected optics. The root mean square (RMS) of the residual aberrations was ∼0.02 μm on average for a 6-mm pupil diameter. The Michelson contrast (Michelson, 1927) of the images captured by the CCD camera in each condition was calculated to compare the contrast degradation produced by real aberrations mapped on the DM or by convolution with the same set of aberrations.

Subjects

Seven young subjects participated in the study, with ages ranging from 28 to 34 years (28.41 ± 1.60). Spherical errors ranged between +0.75 and −3.40 D (1.34 ± 1.90 D), and astigmatism was ≤ −1.25 D in all cases. All participants were acquainted with the nature and possible consequences of the study and provided written informed consent. All protocols met the tenets of the Declaration of Helsinki and had been previously approved by the Spanish National Research Council (CSIC) Ethical Committee.

Experimental protocol

Measurements on subjects took place in two different experimental sessions (seven days apart). In the first session, the HOAs were measured in Near-infrared (NIR) light. In the second session, VA was measured under different conditions. In all measurements, subjects were stabilized using a dental impression mounted on an x-y-z stage. The eye's pupil was aligned to the optical axis of the instruments using the line of sight as a reference. Pupil centration was verified before each trial and between conditions. Also, all measurements were performed monocularly, in a darkened room, under cycloplegia (tropicamide 1%, two drops 10 minutes before the beginning of the experiment and one drop after one hour), to dilate the subject's pupil and minimize the effects of accommodation during the measurements. All measurements were obtained for 6-mm pupil diameters.

Ocular aberration measurements

The best subjective focus was initially searched by the subject while viewing a Maltese cross projected on the DMD at the reference wavelength of 555 nm. Then, the subject's aberrations (HOAs) were measured with the HS wavefront sensor and corrected in a closed loop at 880 nm. The subject was asked again to adjust the Badal system position that provided the best subjective focus for this AO-corrected condition. Each measurement was repeated at least five times per condition.

VA measurements

VA was measured following similar protocols to those described in previous studies at best subjective focus for 555 nm or WL (Marcos et al., 2008; de Gracia et al., 2009). Four different conditions for VA were tested: (a) natural aberrations (with the AO system correcting only the aberrations of the system) with a high-contrast stimulus in monochromatic light (555 nm); (b) same as Condition 1, but with the stimulus illuminated in WL; (c) natural aberrations corrected with DM and a simulated convolved stimulus, degraded by the natural aberrations of the subject, in monochromatic light (555 nm); and (d) same as Condition 3, but with the stimulus illuminated in WL. Conditions are represented in Figure 1. VA measurements were performed

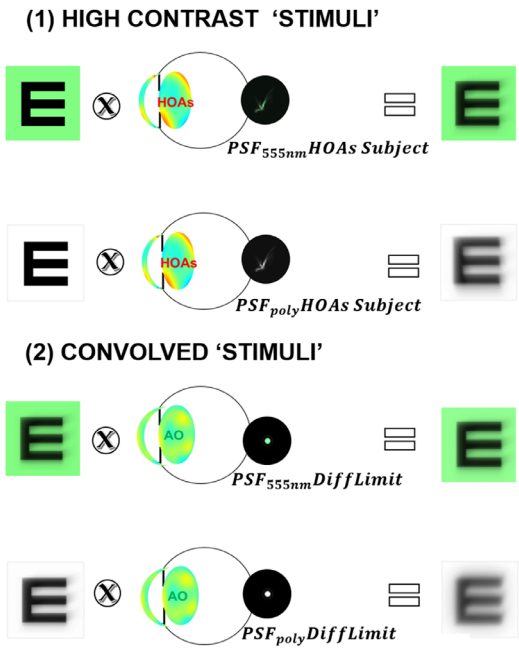

Figure 1. Illustration of the conditions tested computationally and in patients: (1) high-contrast E-letter degraded with a monochromatic (555 nm) or polychromatic (white) PSFs calculated from the subject's aberrations and (2) convolved E-letter degraded with diffraction-limited PSF both in monochromatic (555 nm) or polychromatic light.

using an adaptive QUEST algorithm consisting of an eight alternative forced-choice (Ehrenstein & Ehrenstein, 1999) procedure of tumbling E-letters programmed in the MATLAB psychtoolbox (Brainard, 1997; Pelli, 1997; M Kleiner, 2007) to calculate the sequence of the presented stimulus (letter size and orientation) in the test following the subject's response. The QUEST routine for each VA measurement consisted of 40 trials, and each one was presented for 0.5 seconds. The measurement was discarded if convergence was not reached and the task was repeated three times per condition. VA was expressed in terms of logMAR VA (logMAR = −log10(decimal VA)) (Holladay, 1997). Aberrations were monitored throughout the experiment before every VA measurement to ensure that each trial was performed under the desired state of aberration correction. The total duration of the experiment was around 1.5 hours.

Simulation of the effects of chromatic aberration

We computed the polychromatic PSF considering a polychromatic source image as a sum of a set of monochromatic PSFs for a representative selection of wavelength (Marcos et al., 1999). The sampling interval of the spectrum was from 450 to 800 nm, in 50-nm steps. In previous studies, the analysis was performed with different sampling intervals (1, 10, and 50 nm), and it was concluded that an interval of 50 nm was suitable for typical eye aberrations (Font et al., 1994). Each PSF was weighted with the luminance L(λ) of the polychromatic source (WL) (Ravikumar et al., 2008; Watson, 2015) and the CIE photonic luminosity function V(λ) at the corresponding wavelength (Stockman et al., 1994). The polychromatic PSF was obtained as the weighted linear sum of the monochromatic PSFs (Equation 2). The PSFs for all monochromatic wavelengths were computed using the measured HOAs in IR, given that HOAs do not vary significantly with wavelength (Marcos et al., 1999) and the chromatic difference of focus, obtained from the measured longitudinal chromatic aberration (LCA). We assumed the best focus at 555 nm, and the defocus Zernike coefficients for other wavelengths were adjusted according to the psychophysical chromatic difference of focus reported by Vinas et al. (2015) in the 450- to 800-nm range.

$$PSF_{poly\,(x,y)} = \int PSF_{(x,y,\lambda_{450nm-800nm})} \cdot L\,(\lambda) \cdot V\,(\lambda)\; d\lambda \quad (2)$$

$$Image = PSF_{poly} \otimes Object \quad (3)$$

The same conditions of the experimental measurements in subjects were reproduced in the computational simulations, as illustrated in Figure 1: (a) High-contrast E-letter targets were simulated to be degraded with natural aberrations with a monochromatic $PSF_{555\ nm}$ and with a polychromatic PSF_{poly} light (in this condition, an optical blur was evaluated; Equation 3). (b) Additionally, convolved E-letter targets were simulated to be degraded by diffraction limit only (AO simulation), with monochromatic $PSF_{555\ Diff\ Limit}$ and with polychromatic $PSF_{poly\ Diff\ Limit.}$ The size of the E-letter used in this stimulus was 45 pixels, which is equivalent to a VA of 0.3 logMAR.

Data analysis

The image quality metric to quantify the optical quality of computer-simulated and experimental images of an E-letter was the correlation coefficient, calculated as the 2-D correlation of the images in each condition with the high-contrast E-letter image as the reference (Vinas, Benedi-Garcia, et al., 2019).

Statistical analysis was performed with SPSS software (IBM SPSS Statistics 27; SPSS, Inc., Chicago, IL, USA). For measurements in subjects, VA values were compared across conditions (natural aberrations and convolved stimulus; monochromatic and polychromatic light). For E-letter stimuli, the 2-D correlation metric was compared across conditions (natural aberration and simulated convolution; monochromatic and polychromatic). In all cases, the Shapiro–Wilk test was performed to test for normality.

A nonparametric test (Wilcoxon signed ranks test) was performed to evaluate statistical differences between conditions for VA and simulations. In addition, the different conditions for the 2-D correlation metric and VA were correlated (Pearson or Spearman's ρ test) with VS (natural aberrations or convolved stimuli, both for monochromatic and polychromatic).

Results

Wavefront aberrations (HOAs) and VS

Figure 2 shows wave aberration maps for natural HOAs and residual HOAs after AO correction (top panels), and through-focus VS (bottom panel) for all subjects (6-mm pupil diameter). For illustrative purposes, tilt and defocus Zernike terms were set to zero in the wave aberration plots. RMS values for natural HOAs ranged from 0.20 to 0.61 μm, and the corresponding VS in green ranged from 0.38 to 0.18. RMS values following AO correction ranged from 0.05 to 0.11 μm, with the corresponding VS in green from 0.66 to 0.90 (nearly diffraction limited in all subjects).

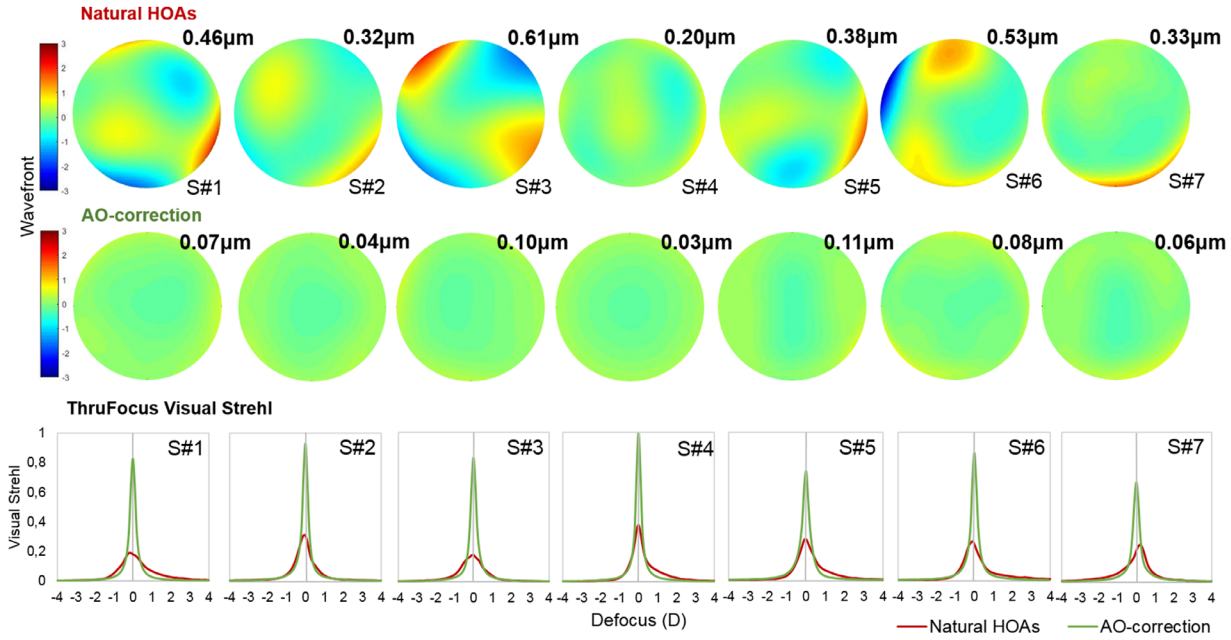

Figure 2. Subject's optical quality. Top row: wave aberrations (third order and higher) under natural conditions, with the corresponding RMS value at the top. Central row: wave aberrations under closed-loop AO correction. Bottom row: through-focus visual Strehl for natural aberrations (red line) and best AO correction during visual acuity measurements (green line). Data are for 6-mm pupil size.

Experimental convolved images versus optical blur

Figure 3A shows the results for the on-bench study, where stimuli were degraded by the aberrations mapped on the DM (columns 3 and 5) or by convolution (columns 2, 4, and 6) and projected through a diffraction-limited system (row 1) and through natural aberrations (of subjects S1–S3). The images were captured on the CCD camera of the artificial eye (zero chromatic aberration) using monochromatic (555 nm) and polychromatic (WL) illumination. The reference stimulus (column 1) corresponds to a 100-pixel size E-letter, equivalent to a 0.70 logMAR VA.

Figure 3B shows the values of the Michelson contrast of the retinal image for each tested condition in the on-bench diffraction limit system and through aberrated optics. Estimations were done studying the vertical profiles of the E-letter image. The discrepancy in the contrast between the simulated images degraded by convolution imaged through diffraction-limited optics and high-contrast images through the wave aberrations imposed in the DM were 3% and 5% for a flat wavefront (DL) for 555 nm and WL, respectively, and 6% and 12% on average across subjects (S1–S3) for 555 nm and WL, respectively. This same procedure was repeated for low-order aberrations (defocus and astigmatism at different angles), as reported by Cheng et al. (2010).

As in the previous report, we found a high similarity between convolved and real images, with average contrast differences within 2% and 3% for 555 nm and WL, respectively.

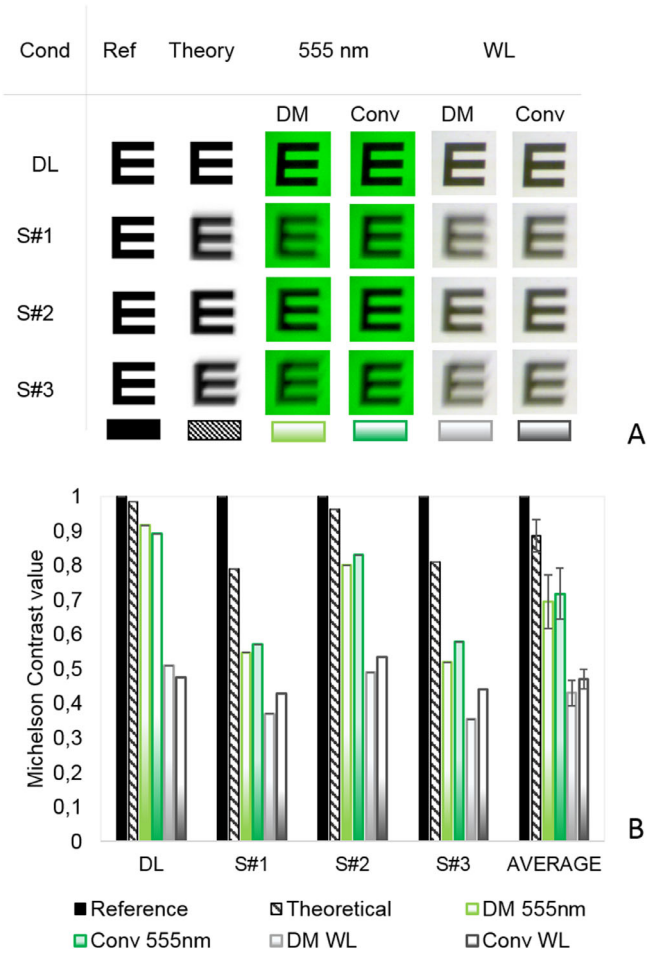

Figure 3. (A) Comparison of images of an E-letter (100 pixels, 0.33 degrees angular subtend) stimulus in optical simulations and captured with the CCD camera (at the retinal plane of an artificial eye). Column 1: high-contrast reference image (Ref). Column 2: computer-simulated image, calculated by convolution of the original image with the subject's aberrations and seen through diffraction-limited optics (Theory). Column 3: high-contrast image projected through an artificial eye with natural aberrations induced on a DM, in green light. Column 4: convolved image projected through diffraction-limited optics (Conv). Column 5: as in column 3, with white light. Column 6: as in column 4, with white light (WL). (B) Michelson contrast value measured according to the maximum and minimum grayscale values along a central vertical profile in the image for the conditions shown in panel A (legend as indicated by the rectangular squares in the bottom of A). The simulations and experimental on-bench measurements (A) and contrast analysis (B) were performed for a diffraction-limited (DL) artificial eye and aberrations of three subjects enrolled in the study (S1, S2, and S3).

VA with real aberrations and convolved images

Figure 4 shows the logMAR VA in the seven measured subjects for all conditions. The average VA under natural HOAs was -0.04 ± 0.01 (555 nm, light green squares) and 0.01 ± 0.02 (WL, light gray squares), resulting in a difference of -0.05 ± 0.01 logMAR between monochromatic and polychromatic illuminations. The average VA using convolved stimuli was 0.04 ± 0.02 (555 nm, dark green squares) and 0.14 ± 0.04 (WL, dark gray squares), resulting in a difference of -0.10 ± 0.01 logMAR between monochromatic and polychromatic illuminations. VA was therefore systematically worse for convolved stimuli. The difference in VA with natural HOAs and with convolved stimulus was larger in polychromatic light (-0.13 ± 0.02 logMAR) than in monochromatic light (-0.06 ± 0.01 logMAR). These differences in logMAR are equivalent to three letters in monochromatic illumination ($p = 0.01$) and one complete line + one letter in polychromatic light ($p = 0.02$) in a clinical

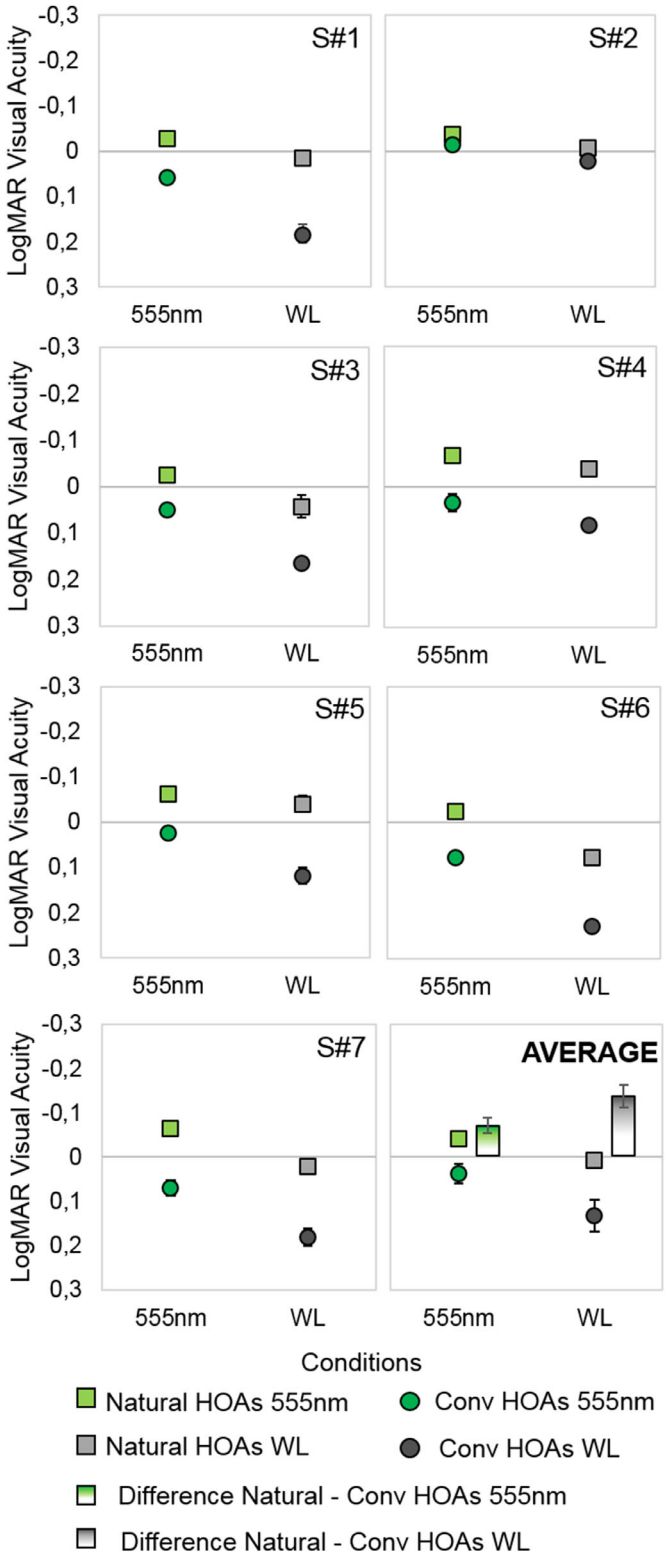

Figure 4. Visual acuity (symbols) for all subjects and average for the following conditions: high-contrast stimulus and natural aberrations in green light (light green squares); convolved stimulus through natural aberrations, in green light (dark green circles); high-contrast stimulus and natural aberrations in white light (light gray squares); and convolved stimulus through natural aberrations, in white light (dark gray circles). The gradient bars in the average plot represent the VA differences between measurements with natural aberrations and convolved images in monochromatic (green bar) and white light (gray bar), on average. The error bars in the plots for individual subjects stand for the standard deviation of the repeated measurements (in most cases smaller than the symbol). The error bars in the average plot stand for standard deviations across subjects.

chart (Bailey & Lovie-Kitchin, 2013). The error bars in individual data represent the standard deviation of the three repeated measurements per condition and were ≤ 0.02 logMAR (high repeatability) in all cases.

The correlation between VA and visual quality (VS) was evaluated in all conditions. VA and VS were statistically significantly correlated for natural aberrations at 555 nm ($r = 0.73$, $p = 0.02$). However, VA and VS were not significantly correlated for convolved images at 555 nm ($r = 0.52$, $p = 0.18$), nor in white light for either natural aberrations or convolved images ($r = 0.65$, $p = 0.12$).

Simulations of mono- and polychromatic effects on retinal images

Figure 5 shows the estimated retinal image quality (2-D correlation metric) for simulated images using the subject's aberrations (bars, left y-axis) and the VA in the same subjects (symbols and dashed lines, right y-axis) for four different conditions: high-contrast green stimuli degraded by a monochromatic $PSF_{555\ nm}$ (light green bar/squares); high-contrast white stimuli degraded by polychromatic PSF_{poly} (light gray bar/square); green stimuli convolved with $PSF_{555\ nm}$, followed by convolution with diffraction-limited optics, $PSF_{555\ nm\ Diff\ Limit}$ (dark green bar/circle); and same convolved stimulus, followed by convolution with diffraction-limited optics, polychromatic $PSF_{poly\ Diff\ Limit}$ (dark green bar/circle). The 2-D correlation metric difference between real and convolved images was 0.01 in monochromatic green light and 0.04 in white light, with this difference being statistically significant ($p = 0.02$). There was a high correlation between 2-D correlation metric values for natural and convolved images in 555 nm ($p < 0.001$) but not in white light ($p = 0.76$).

We did not find a correlation between VA with natural aberrations and VA with convolved images at 555 nm ($p = 0.07$) or in white light ($p = 0.54$). However, there was a high correspondence between the predictions from optical simulations (2-D correlation metric) and VA in all conditions ($r = 0.60$, $p < 0.001$), considering all conditions and subjects, with

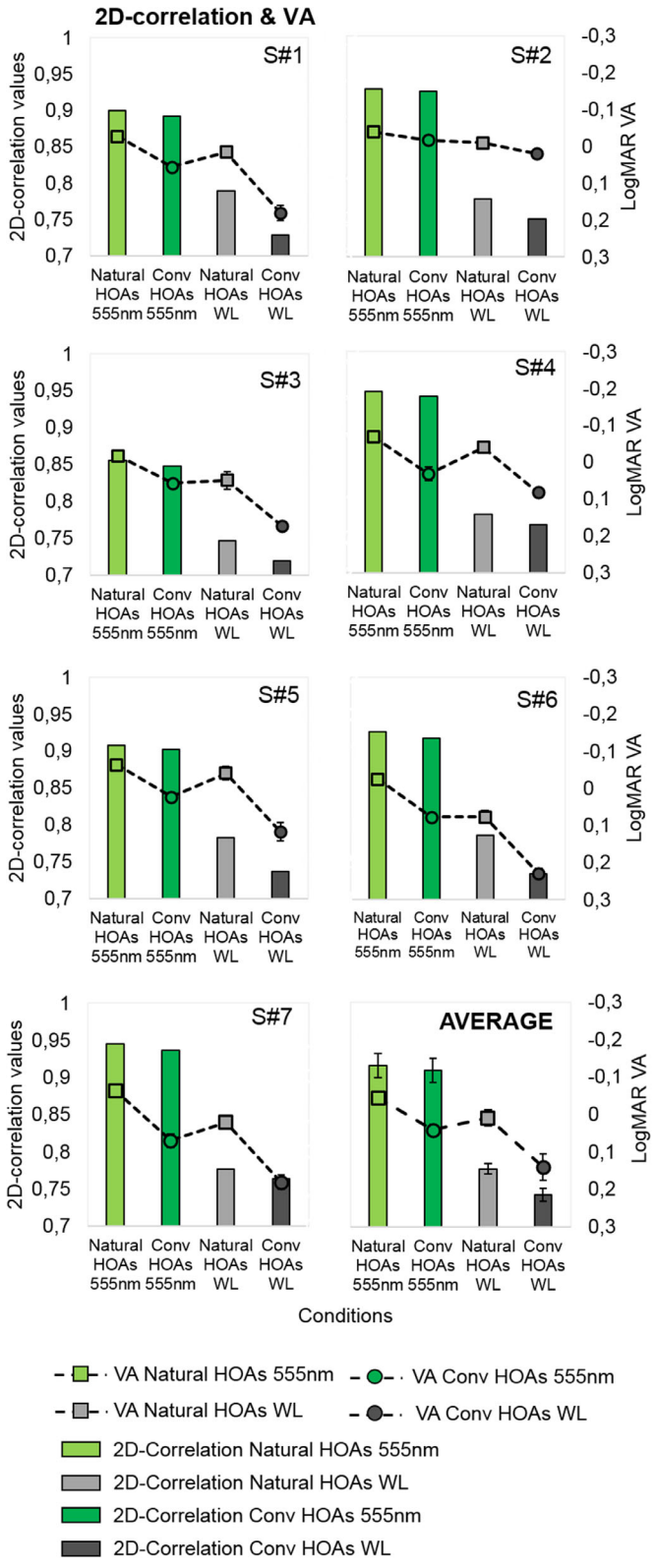

Figure 5. Optical quality (2-D correlation metric, left axis) and visual quality (logMAR VA, right-axis) for the following conditions: high-contrast stimulus and natural aberrations in green light (light green bar/square); convolved stimulus through natural aberrations, in green light (dark green bar/circle); high-contrast stimulus and natural aberrations in white light (light gray bar/square); and convolved stimulus through natural aberrations, in white light (dark gray bar/circle). Dashed lines have been included to facilitate comparison of VA across conditions. The error bars in the plots for individual subjects stand for the standard deviation of the repeated measurements (in most cases smaller than the symbol). The error bars in the average plot stand for standard deviations across subjects.

a normalized distribution of the residuals in the regression. The highest correlation between optical quality and VA was found for natural aberrations and monochromatic light ($r = 0.73$, $p = 0.02$) and the lowest with convolved images in white light ($r = 0.65$, $p = 0.12$).

Discussion

Convolved stimuli to simulate the degradation assessed by HOAs are frequently used in studies aiming at understanding the impact of blur on visual performance. A systematic underestimation of the visual performance with the simulated stimuli, in comparison with real optical degradation, has been reported (de Gracia et al., 2009; Ohlendorf et al., 2011), although the causes for the discrepancies were left unexplained. In the current study, we addressed this comparison in both an artificial eye and seven real subjects, using AO to control and correct the aberrations of the eye and the system, therefore minimizing the impact of double image degradation. Also, having a polychromatic AO system allows evaluating the chromatic effects for both optical blur and convolved stimuli.

We confirmed degradation of VA measured with stimulus degraded by convolution, although this was much lower than in previous reports. For example, a previous study reported a 50% discrepancy in the VA measurement with optical or simulated astigmatic degradation (Ohlendorf et al., 2011), as opposed to 8% for high-order aberration degradation in the current study at 555 nm and 26% in WL.

Approximations in the computational simulation of the convolved image have often been raised as a potential cause for the discrepancy. Differences in the PSF computed using Fourier optics, the Fraunhofer and Fresnel approximation, and the exact solutions have been reported, under certain conditions (i.e., out of focus) (Barbero & Marcos, 2008). However, our experiments in an artificial eye (without chromatic aberration, achromatic lens doublet) predict minimal differences between contrast degradation with real optics and convolved stimuli (taking into account the double diffraction): 6% at 555 nm and 12% in WL for

RMS for HOAs ranging from 0 to 0.61 μm. These values suggest that relying on assumptions in the computation of retinal images using convolutions is not a significant source of discrepancy in monochromatic or polychromatic light, particularly in the absence of chromatic aberration.

Although convolved stimuli projected under AO correction and high-contrast stimuli projected through aberrations induced by DM show some quantitative differences $\leq 12\%$ (Figure 3), the fact that the differences are minimal when the induced aberrations were defocus or astigmatism suggest that those discrepancies may be associated with a slightly lower compliance of the deformable mirror or imaging system when working with higher-order aberrations.

Experiments with both the artificial eye and real eyes were performed using monochromatic/polychromatic stimuli, although only monochromatic aberrations were used in the convolution. The same conditions experienced by the subjects were tested by computer simulation. The chromatic aberration of the instrument and the focusing lens of the artificial eye was expected to be negligible, while the eye is known to suffer from significant amounts of chromatic aberration (Thibos et al., 1990; Thibos et al., 1992; Rynders et al., 1995).

However, in computer simulations and real eye measurements, including chromatic resulted in systematic deterioration of the optical/visual quality with convolved images, with respect to the natural condition. This deterioration of VA with convolved images had been found in previous studies in polychromatic illumination (de Gracia et al., 2009), but so far, reports were not conclusive whether this decrease also occurred with monochromatic illumination. The current study confirms that the optical degradation of stimuli simulated by convolution and projected on the retina through diffraction-limited optics is significantly higher in polychromatic light than in monochromatic light ($p < 0.05$).

This finding supports our hypothesis that chromatic aberrations play an important role in the degradation of the simulated stimulus seen under corrected monochromatic aberrations. Although chromatic and monochromatic aberrations have been shown to interact to improve retinal image or perception under natural conditions, the effect of chromatic aberrations is highly detrimental in diffraction-limited eyes (McLellan et al., 2002; Benedi-Garcia et al., 2021), as it occurs in experiments in which convolved stimuli with the aberrations of the subjects are observed through corrected optical aberrations with AO to avoid double degradation.

Several previous studies have evaluated the impact of chromatic aberrations (both transverse chromatic aberration (TCA) and LCA) in an eye in the presence of monochromatic aberrations or corrected for monochromatic aberrations (Campbell & Gubisch 1967; Marcos et al., 1999; Yoon & Williams, 2002). In the simulations shown earlier, only the LCA was considered. LCA is fairly constant across subjects, ~2-D between the two ends of the visible spectrum (400–700 nm), in phakic subjects (Wald & Griffin, 1947; Bedford & Wyszecki, 1957; Thibos et al., 1990; Vinas et al., 2015). In contrast, the reported TCA varies largely in the population, in both magnitude and orientation (Ogboso & Bedell, 1987; Simonet & Campbell, 1990; Thibos et al., 1990). The TCA in five of the seven subjects participating in the current study was available from previous work (Aissati et al., 2020), and it was -0.20 ± 0.10 arcmin on average in the vertical direction and 1.54 ± 0.10 arcmin in the horizontal direction. We recalculated the MTFs in all subjects for the four conditions of the study incorporating both the individual measurements of monochromatic aberrations and LCA and TCA, using the method described by Marcos et al. (1999). Unlike other studies (Marcos et al., 1999), and likely due to the small magnitude of the foveal TCA in our subjects, we did not find that incorporating TCA further reduced significantly the MTF under natural aberrations or diffraction-limited optics. Given that the effect seemed to be driven primarily by LCA, we limited the analysis to calculations using LCA only.

The SCE has often been invoked as a potential factor leading to discrepancies in the simulated or real retinal image quality, as the pupil apodization may lead to a smaller effective pupil and therefore improved effective optical quality with natural optics. In a previous study (Aissati et al., 2020), we measured the peak positions of the SCE in a subset of the subjects of the present study (five of the seven subjects). As those measurements were obtained from a reflectometric technique (laser ray tracing measurements in green light) (Marcos & Burns, 2009), we did not attempt to use the width of the measured SCE function in the simulations, as there are known differences in the width of the psychophysical and reflectometric SCE (Marcos & Burns, 1999). We therefore assumed a value of 0.1 mm^{-2} for the SCE width. On average, for these subjects, the SCE peak location lies at 1.20 ± 0.34 mm nasally and -0.34 ± 0.39 mm inferiorly from the geometric center of the pupil. The simulations incorporating the SCE were analyzed in terms of VS. We found an average increase of only 5% in VS when the SCE was included. We correlated the decentration of the SCE peak with the discrepancy in the VA measurements from simulations and real aberrations and did not find any statistical trend ($p > 0.05$). This analysis suggests that the SCE does not play a significant role in the simulated retinal images and therefore in differences between VA measured through natural aberrations and convolved stimuli (in green light).

Experiments were conducted under cycloplegia, minimizing the presence of fluctuations of

accommodation. However, while in the optically degraded condition, residual accommodation (if still present) may interact favorably with the natural aberrations, those possible favorable interactions are by no means possible with the convolved stimuli displayed on the screen residual aberrations after AO correction of aberrations. Also, it has been suggested that scattering in the ocular media may combine differently with aberrated or diffraction-limited optics, which could be an additional source of discrepancy (Pérez et al., 2009) between stimuli observed through the natural optics and convolved images observed through AO-corrected optics (but still subject to diffraction). However, we did not find a significant correlation between the difference in VA with natural aberrations and simulated images (in green light) as a function of residual aberrations in the AO correction ($p > 0.05$).

Conclusions

Convolved stimuli are widely used to assess the effects of low- and high-order aberrations and optical corrections on visual performance. To our knowledge, this study presents the first direct comparison of visual performance under high-order natural aberrations and that obtained with simulated stimulus by convolution in monochromatic and polychromatic illumination. The use of adaptive optics to minimize the impact of the subject's natural aberrations has allowed us to perform the comparison in the best comparable conditions, resulting in a better match between natural aberrations and the degradation by simulation of convolved images than previous reports. The systematic decrease in visual performance measured with visual acuity and retinal image quality by simulation with convolved stimulus appears to be primarily associated with the lack of favorable interactions between chromatic and monochromatic aberrations (Marcos et al., 1999; McLellan et al., 2002; Ravikumar et al., 2006; Benedi-Garcia et al., 2021). Optical simulations and visual acuity experiments in real eyes support the hypothesis that a larger degradation with convolved stimuli (observed through corrected optics) in comparison with natural viewing occurs most noticeably in polychromatic light. Besides additional confirmation of the interactive effects of chromatic and monochromatic aberrations, this study has practical implications in studies that use convolved images in psychophysical studies.

Keywords: ocular aberrations, convolved images, polychromatic optical quality, retinal optical quality, optical quality metrics, adaptive optics

Acknowledgments

Supported by the Spanish Government (FIS2017 84753R, PID2020-115191RB-I00) to SM; Spanish Government Predoctoral (Grant FPU16/01944) to SA; H2020 Marie Sklodowska-Curie Actions (H2020 MSCA IF GF 2019 MYOMICRO 893557) to MV; European Research Council (ERC-2018-ADG SILKEYE 833106), NIH NIE P30EY 001319; and Unrestricted Funds Research to Prevent Blindness to SM.

Commercial relationships: none.
Corresponding author: Sara Aissati.
Email: sara.elaissati@csic.es.
Address: Instituto de Óptica CSIC. Serrano 121, 28006, Madrid, Spain.

References

Aissati, S., Vinas, M., Benedi-Garcia, C., Dorronsoro, C., & Marcos, S. (2020). Testing the effect of ocular aberrations in the perceived transverse chromatic aberration. *Biomedical Optics Express, 11*(8), 4052–4068, [Article].

Anstis, S., & Cavanagh, P. (1983). A minimum motion technique for judging equiluminance. In J. D. Mollon, & L. T. Sharpe (Eds.), *Colour Vision: Psychophysics and Physiology* (pp. 155–166). London: Academic Press.

Applegate, R. A., Ballentine, C., Gross, H., Sarver, E. J., & Sarver, C. A. (2003). Visual acuity as a function of Zernike mode and level of root mean square error. *Optometry and Vision Science, 80*(2), 97–105, https://journals.lww.com/optvissci/Abstract/2003/02000/Visual_Acuity_as_a_Function_of_Zernike_Mode_and.5.aspx.

Applegate, R. A., & Lakshminarayanan, V. (1993). Parametric representation of Stiles–Crawford functions: Normal variation of peak location and directionality. *Journal of the Optical Society of America A, 10*(7), 1611–1623. [PubMed]

Applegate, R. A., Marsack, J. D., Ramos, R., & Sarver, E. J. (2003). Interaction between aberrations to improve or reduce visual performance. *Journal of Cataract & Refractive Surgery, 29*(8), 1487–1495, https://journals.lww.com/jcrs/Abstract/2003/08000/Interaction_between_aberrations_to_improve_or.26.aspx.

Applegate, R. A., Sarver, E. J., & Khemsara, V. (2002). Are all aberrations equal? *Journal of Refractive Surgery, 18*(5), S556–S562, https://journals.healio.com/doi/abs/10.3928/1081-597X-20020901-12.

Artal, P. (1990). Calculations of two-dimensional foveal retinal images in real eyes. *Journal of the Optical Society of America A, 7*(8), 1374–1381. [PubMed]

Artal, P., Marcos, S., Navarro, R., & Williams, D. R. (1995). Odd aberrations and double-pass measurements of retinal image quality. *Journal of the Optical Society of America A, 12*(2), 195–201. [PubMed]

Atchison, D. A., Joblin, A., & Smith, G. (1998). Influence of Stiles–Crawford effect apodization on spatial visual performance. *Journal of the Optical Society of America A, 15*(9), 2545–2551, [Article].

Atchison, D. A., Marcos, S., & Scott, D. H. (2003). The influence of the Stiles–Crawford peak location on visual performance. *Vision Research, 43*(6), 659–668, [Article].

Bailey, I. L., & Lovie-Kitchin, J. E. (2013). Visual acuity testing. From the laboratory to the clinic. *Vision Research, 90*, 2–9.

Barbero, S., & Marcos, S. (2008). Analysis of the optical field on the human retina from wavefront aberration data. *Journal of the Optical Society of America A, 25*(9), 2280–2285, [Article].

Bedford, R. E., & Wyszecki, G. (1957). Axial chromatic aberration of the human eye. *Journal of the Optical Society of America A, 47*(6), 564–565.

Benedi-Garcia, C., Vinas, M., Dorronsoro, C., Burns, S. A., Peli, E., & Marcos, S. (2021). Vision is protected against blue defocus. *Scientific Reports, 11*(1), 352, [Article].

Brainard, D. H. (1997). The psychophysics toolbox. *Spatial Vision, 10*(4), 433–436, [PubMed].

Burns, S. A., & Marcos, S. (2000). Evaluating the role of cone directionality in image formation. Paper presented at the Vision Science and its Applications, Santa Fe, New Mexico, 22–25, https://opg.optica.org/abstract.cfm?uri=vsia-2000-FA2.

Burton, G. J., & Haig, N. D. (1984). Effects of the Seidel aberrations on visual target discrimination. *Journal of the Optical Society of America A, 1*(4), 373–385, [PubMed].

Campbell, F. W., & Gubisch, R. W. (1967). The effect of chromatic aberration on visual acuity. *The Journal of Physiology, 192*(2), 345–358, [Article].

Charman, W. N. (1991). Wavefront aberration of the eye: A review. *Optometry and Vision Science: Official Publication of the American Academy of Optometry, 68*(8), 574–583, [PubMed].

Cheng, X., Bradley, A., Ravikumar, S., & Thibos, L. N. (2010). Visual impact of Zernike and Seidel forms of monochromatic aberrations. *Optometry and Vision Science, 87*(5), 300–312. [Article].

Dalimier, E., Dainty, C., & Barbur, J. (2008). Effects of higher-order aberrations on contrast acuity as a function of light level. *Journal of Modern Optics, 11*: 24–29.

de Gracia, P., Dorronsoro, C., Sawides, L., Gambra, E., & Marcos, S. (2009). Experimental test of simulated retinal images using adaptive optics. Paper presented at the Frontiers in Optics 2009/Laser Science XXV/Fall 2009 OSA Optics & Photonics Technical Digest, San Jose, California, https://opg.optica.org/abstract.cfm?URI=AOPT-2009-JWB4.

de Gracia, P., Marcos, S., Mathur, A., & Atchison, D. A. (2011). Contrast sensitivity benefit of adaptive optics correction of ocular aberrations. *Journal of Vision, 11*(12), 5–5, doi:10.1167/11.12.5.

Delori, F. C., Webb, R. H., & Sliney, D. H. (2007). Maximum permissible exposures for ocular safety (ANSI 2000), with emphasis on ophthalmic devices. *Journal of the Optical Society of America A, 24*(5), 1250–1265, [PubMed].

Ehrenstein, W. H., & Ehrenstein, A. (1999). Psychophysical methods. In U. Windhorst, & H. Johansson (Eds.), *Modern Techniques in Neuroscience Research* (pp. 1211–1241). Berlin, Heidelberg: Springer Berlin Heidelberg.

Flamant, F. (1955). Étude de la répartition de lumière dans l'image rétinienne d'une fente [Study of light distribution in the retinal image of a slit.]. *Revue d'Optique Theorique et Instrumentale, 34*, 433–459.

Font, C., Escalera, J. C., & Yzuel, M. J. (1994). Polychromatic point spread function: Calculation accuracy. *Journal of Modern Optics, 41*(7), 1401–1413, [Article].

Goodman, J. W. (1996). Introduction to Fourier optics. New York: McGraw-Hill.

He, J. C., Marcos, S., & Burns, S. A. (1999). Comparison of cone directionality determined by psychophysical and reflectometric techniques. *Journal of the Optical Society of America A, 16*(10), 2363–2369, [Article].

Holladay, J. T. (1997). Proper method for calculating average visual acuity. *Journal of Refractive Surgery, 13*(4), 388–391.

Iskander, D. R. (2006). Computational aspects of the visual Strehl ratio. *Optometry and Vision Science, 83*(1), 57–59, https://journals.lww.com/optvissci/Abstract/2006/01000/Computational_Aspects_of_the_Visual_Strehl_Ratio.15.aspx.

Jaeken, B., & Artal, P. (2012). Optical quality of emmetropic and myopic eyes in the periphery measured with high-angular resolution. *Investigative Ophthalmology & Visual Science, 53*(7), 3405–3413. [Article].

Kleiner, M., Brainard, D. H., Pelli, D., Ingling, A., Murray, R., & Broussard, C (2007). What's new in Psychtoolbox-3. *Perception, 36*, 1–16.

Legras, R., Chateau, N., & Charman, W. N. (2004). Assessment of just-noticeable differences for refractive errors and spherical aberration using visual simulation. *Optometry and Vision Science, 81*(9), 718–728, https://journals.lww.com/optvissci/Abstract/2004/09000/Assessment_of_Just_Noticeable_Differences_for.17.aspx.

Marcos, S., Barbero, S., & Jiménez-Alfaro, I. (2005). Optical quality and depth-of-field of eyes implanted with spherical and aspheric intraocular lenses. *Journal of Refractive Surgery, 21*(3), 223–235, https://journals.healio.com/doi/abs/10.3928/1081-597X-20050501-05.

Marcos, S., Benedí-García, C., Aissati, S., Gonzalez-Ramos, A. M., Lago, C. M., & Radhkrishnan, A., . . .Vinas, M. (2020). VioBio lab adaptive optics: technology and applications by women vision scientists. *Ophthalmic and Physiological Optics, 40*(2), 75–87, [PubMed].

Marcos, S., & Burns, S. A. (1999). Cone spacing and waveguide properties from cone directionality measurements. *Journal of the Optical Society of America A, 16*(5), 995–1004, [PubMed].

Marcos, S., & Burns, S. A. (2009). Cone directionality from laser ray tracing in normal and LASIK patients. *Journal of Modern Optics, 56*(20), 2181–2188.

Marcos, S., Burns, S. A., Moreno-Barriusop, E., & Navarro, R. (1999). A new approach to the study of ocular chromatic aberrations. *Vision Research, 39*(26), 4309–4323, [PubMed].

Marcos, S., Sawides, L., Gambra, E., & Dorronsoro, C. (2008). Influence of adaptive-optics ocular aberration correction on visual acuity at different luminances and contrast polarities. *Journal of Vision, 8*(13), 1–1, doi:10.1167/8.13.1.

Marcos, S., Werner, J. S., Burns, S. A., Merigan, W. H., Artal, P., & Atchison, D. A., . . .Sincich, L. C. (2017). Vision science and adaptive optics, the state of the field. *Vision Research, 132*, 3–33, [PubMed].

McLellan, J. S., Marcos, S., Prieto, P. M., & Burns, S. A. (2002). Imperfect optics may be the eye's defence against chromatic blur. *Nature, 417*(6885), 174–176, [PubMed].

Michelson, A. A. (1927). *Studies in optics*. Chicago, IL: University of Chicago Press.

Ogboso, Y. U., & Bedell, H. E. (1987). Magnitude of lateral chromatic aberration across the retina of the human eye. *Journal of the Optical Society of America A, 4*(8), 1666–1672, [PubMed].

Ohlendorf, A., Tabernero, J., & Schaeffel, F. (2011). Visual acuity with simulated and real astigmatic defocus. *Optometry and Vision Science, 88*(5), 562–569, https://journals.lww.com/optvissci/Fulltext/2011/05000/Visual_Acuity_with_Simulated_and_Real_Astigmatic.4.aspx.

Peli, E., & Lang, A. (2001). Appearance of images through a multifocal intraocular lens. *Journal of the Optical Society of America A, 18*(2), 302–309, [PubMed].

Pelli, D. G. (1997). The VideoToolbox software for visual psychophysics: Transforming numbers into movies. *Spatial Vision, 10*(4), 437–442, [PubMed].

Pérez, G. M., Manzanera, S., & Artal, P. (2009). Impact of scattering and spherical aberration in contrast sensitivity. *Journal of Vision, 9*(3), 19–19, doi:10.1167/9.3.19.

Raphael, S., & MacLeod, D. I. A. (2011). Mesopic luminance assessed with minimum motion photometry. *Journal of Vision, 11*(9), 14–14, doi:10.1167/11.9.14.

Ravikumar, S., Bradley, A., & Thibos, L. N. (2006). Do monochromatic aberrations protect the eye against chromatic blur? *Investigative Ophthalmology & Visual Science, 47*(13), 1505–1505.

Ravikumar, S., Thibos, L. N., & Bradley, A. (2008). Calculation of retinal image quality for polychromatic light. *Journal of the Optical Society of America A, 25*(10), 2395–2407, [Article].

Rynders, M., Lidkea, B., Chisholm, W., & Thibos, L. N. (1995). Statistical distribution of foveal transverse chromatic aberration, pupil centration, and angle ψ in a population of young adult eyes. *Journal of the Optical Society of America A, 12*(10), 2348–2357, [Article].

Santamaría, J., Artal, P., & Bescós, J. (1987). Determination of the point-spread function of human eyes using a hybrid optical–digital method. *Journal of the Optical Society of America A, 4*(6), 1109–1114, [Article].

Sawides, L., de Gracia, P., Dorronsoro, C., Webster, M., & Marcos, S. (2011a). Adapting to blur produced by ocular high-order aberrations. *Journal of Vision, 11*(7), 21–21, doi:10.1167/11.7.21.

Sawides, L., de Gracia, P., Dorronsoro, C., Webster, M. A., & Marcos, S. (2011b). Vision is adapted to the natural level of blur present in the retinal image. *PLoS ONE, 6*(11), e27031.

Sawides, L., Gambra, E., Pascual, D., Dorronsoro, C., & Marcos, S. (2010). Visual performance with real-life tasks under adaptive-optics ocular

aberration correction. *Journal of Vision, 10*(5), 19–19, doi:10.1167/10.5.19.

Simonet, P., & Campbell, M. C. W. (1990). The optical transverse chromatic aberration on the fovea of the human eye. *Vision Research, 30*(2), 187–206, [PubMed].

Stockman, A., MacLeod, D., & Johnson, N. (1994). Spectral sensitivities of human cones. *Journal of the Optical Society of America A, 10*, 2491–2521, [PubMed].

Thibos, L. N., Applegate, R. A., Schwiegerling, J. T., & Webb, R. (2000). *Standards for reporting the optical aberrations of eyes. vision science and its applications*. Santa Fe, NM: Optical Society of America, [PubMed].

Thibos, L. N., Bradley, A., Still, D. L., Zhang, X., & Howarth, P. A. (1990). Theory and measurement of ocular chromatic aberration. *Vision Research, 30*(1), 33–49, [PubMed].

Thibos, L. N., Ye, M., Zhang, X., & Bradley, A. (1992). The chromatic eye: A new reduced-eye model of ocular chromatic aberration in humans. *Applied Optics, 31*(19), 3594–3600, [PubMed].

van Meeteren, A. (1974). Calculations on the optical modulation transfer function of the human eye for white light. *Optica Acta: International Journal of Optics, 21*(5), 395–412, [Article].

Vinas, M., Aissati, S., Gonzalez-Ramos, A. M., Romero, M., Sawides, L., & Akondi, V., . . .Marcos, S. (2020). Optical and visual quality with physical and visually simulated presbyopic multifocal contact lenses. *Translational Vision Science & Technology, 9*(10), 20. [Article].

Vinas, M., Aissati, S., Romero, M., Benedi-Garcia, C., Garzon, N., & Poyales, F., . . .Marcos, S. (2019). Pre-operative simulation of post-operative multifocal vision. *Biomedical Optics Express, 10*(11), 5801–5817, [Article].

Vinas, M., Benedi-Garcia, C., Aissati, S., Pascual, D., Akondi, V., Dorronsoro, C., . . . Marcos, S. (2019). Visual simulators replicate vision with multifocal lenses. *Scientific Reports, 9*(1), 1539, [Article].

Vinas, M., Dorronsoro, C., Cortes, D., Pascual, D., & Marcos, S. (2015). Longitudinal chromatic aberration of the human eye in the visible and near infrared from wavefront sensing, double-pass and psychophysics. *Biomedical Optics Express, 6*(3), 948–962, [PubMed].

Wald, G., & Griffin, D. R. (1947). The change in refractive power of the human eye in dim and bright light. *Journal of the Optical Society of America A, 37*(5), 321–336, [Article].

Watson, A. B. (2015). Computing human optical point spread functions. *Journal of Vision, 15*(2), 26–26, doi:10.1167/15.2.26.

Yoon, G.-Y., & Williams, D. R. (2002). Visual performance after correcting the monochromatic and chromatic aberrations of the eye. *Journal of the Optical Society of America A, 19*(2), 266–275, [Article].